Arab J Sci Eng (2011) 36:1607–1619
DOI 10.1007/s13369-011-0143-8

RESEARCH ARTICLE - MATHEMATICS

Philip Oladapo Olanrewaju · Oluwole Daniel Makinde

Effects of Thermal Diffusion and Diffusion Thermo on Chemically Reacting MHD Boundary Layer Flow of Heat and Mass Transfer Past a Moving Vertical Plate with Suction/Injection

Received: 15 September 2010 / Accepted: 25 October 2011 / Published online: 10 December 2011

Abstract Analysis is conducted on free convective heat and mass transfer of an incompressible, electrically conducting fluid past a moving vertical plate in the presence of suction and injection with thermal diffusion (Soret) and diffusion-thermo (Dufour) effects. Similarity solutions are obtained using scaling transformations. Using the similarity variables, the governing non-linear partial differential equations are transformed into a set of coupled non-linear ordinary differential equations, which are solved numerically by the shooting iteration technique together with a sixth order Runge–Kutta integration scheme. A comparison with previous work is made and the results are consistent. Numerical calculations of the local skin friction coefficient, the local Nusselt number and the local Sherwood number as well as velocity, temperature and concentration profiles of the fluid, are presented for different physical parameters. It was found that: (i) for fluids with light-medium molecular weight (H_2, air), Dufour and Soret effects should not be neglected; and (ii) the suction and injection parameters largely govern the rate of heat transfer in the boundary layer.

Keywords Free convection · Magneto-hydrodynamics (MHD) · Chemical reaction · Heat and mass transfer · Dufour and Soret effects · Moving porous plate

Mathematics Subject Classification (2010) 76V05 · 80A32 · 80M25 · 92C45 · 92E20

الملخص

يجري تحليلٌ للحمل الحراري الحر ونقل المادة في سائل غير قابل للضغط وموصل للكهرباء في صفيحة عمودية متحركة في ظل وجود شفط وحقن مع انتشار حراري (سوريت) وآثار انتشار حراري (ديوفور). يتم الحصول على حلول تشابه باستخدام تحويلات تغيير المقياس. باستخدام متغيرات التشابه، يتم تحويل المعادلات التفاضلية الجزئية غير الخطية الحاكمة إلى مجموعة من أزواج المعادلات التفاضلية العادية غير الخطية التي يتم حلها عددياً باستخدام تقنية الاستهداف والتكرار مع مخطط تكامل رنجا-كتا من الرتبة السادسة. تمت المقارنة مع أبحاث سابقة وكانت النتائج متسقة معها. يتم عرض حسابات عددية لمعامل احتكاك الجلد المحلي، وعدد نسلت المحلي، وعدد شيروود المحلي، وكذلك لملامح سرعة وحرارة وتركيز السائل بالنسبة لعدة مَعلمات فيزيائية. وجد أنه (i) لا يمكن إهمال آثار ديوفور وسوريت للسوائل ذات الوزن الجزيئي الخفيف – المتوسط (الهواء,H_2)، وأن (ii) وسائط الشفط والحقن تحكم معدل نقل الحرارة في الطبقة المحيطية بشكل كبير.

P. O. Olanrewaju (✉)
Department of Mathematics, Covenant University, Ota, Ogun State, Nigeria
E-mail: oladapo_anu@yahoo.ie

O. D. Makinde
Faculty of Engineering, Cape Peninsula University of Technology, Cape Town, South Africa
E-mail: makinded@cput.za.ca

1 Introduction

Transport of heat through a porous medium is being extensively studied, as understanding the associated transport processes becomes increasingly important. This interest stems from the variety of cases which can be modeled or approximated as transport through porous media, such as packed sphere beds, high performance insulation for buildings, chemical catalytic reactors, grain storage, and many others. Literature concerning convective flow in porous media is abundant, and many representative studies have been published in the past decade [3,8,9,16,20,23,24].

Finding analytical solutions to steady hydromagnetic flow and heat transfer over a stretching surface could be of great benefit to polymer technology and to metallurgy. In particular, many metallurgical processes involve the cooling of continuous strips or filaments by drawing them though a quiescent fluid. In the process of drawing, these strips may be stretched. In the case of annealing and thinning of copper wires, the properties of the final product depend largely on the rate of cooling. By drawing such strips in an electrically conducting fluid subjected to a magnetic field, the rate of cooling can be controlled and final products of desired characteristics are obtainable [4]. Furthermore, in several engineering processes, such as extrusion manufacturing processes and heat treated materials traveling on conveyor belts, the materials possess the characteristics of a moving continuous surface. Steady heat flow on a moving continuous flat surface was first considered by Sakiadis [21] who developed a numerical solution using a similarity transformation. Chiam [5] reported solutions for steady hydromagnetic flow over a surface stretching with a power law velocity.

Makinde [11–14] have investigated magneto-hydrodynamics (MHD) convection in porous medium. A similar problem, involving natural convection about a vertical impermeable flat plate, was tackled by Sparrow and Cess [22]. Yih [25] studied the free convection effect on MHD-coupled heat and mass transfer from a moving permeable vertical surface. Alan and Rahman [1] examined Dufour and Soret effects on mixed hydrogen-air convective flow past a vertical porous flat plate embedded in a porous medium. The onset of double diffusive convection in a two component coupled stress fluid layer with Soret and Dufour effects was investigated by Gaikwad et al. [6], via linear and non-linear stability analysis. Emmanuel et al. [19] studied numerically the effect of thermal-diffusion and diffusion-thermo on combined heat and mass transfer of flows induced by a rotating disk with viscous dissipation and Ohmic heating. Anwar et al. [2] examined the combined diffusion and impedance effects on heat and mass transfer in an electrically-conducting fluid from a vertical stretching surface in a porous medium in the presence of a uniform transverse magnetic field. Numerical simulations of double-diffusive natural convection of water in a partially heated enclosure with Soret and Dufour coefficients around the density maximum were conducted by Nithyadevi and Yang [17]. Olanrewaju [18] explored transient convective flow with radiative heat transfer past a moving flat plate in a binary mixture. Recently, Ibrahim and Makinde [7] studied the combined effects of wall suction and magnetic fields on boundary layer flow with heat and mass transfer over an accelerating vertical plate. The present communication considers the effects of Dufour and Soret diffusion on free convection of a continuously moving porous vertical surface as presented in [7]. The plate is assumed to generate heat uniformly. The effects of heat and mass transfer in the hydromagnetic boundary layer flow of the moving plate, and chemical reaction with Dufour and Soret in the presence of suction/injection, are evaluated numerically. Using scaling transformations, the set of governing equations and the boundary conditions are reduced to non-linear ordinary differential equations with appropriate boundary conditions. The similarity equations are solved numerically by the shooting technique with sixth-order Runge–Kutta integration scheme. Numerical results of the local skin friction coefficient and the local Nusselt number as well as the velocity, temperature and concentration profiles are presented for different physical parameters.

2 Governing Equations

We consider the steady free convective heat and mass transfer flow of a viscous, incompressible, electrically conducting fluid past a moving vertical plate with suction/injection in the presence of thermal diffusion (Soret) and diffusion-thermo (Dufour) effects (see Fig. 1) The non-uniform transverse magnetic field B_0 is imposed along the y-axis. The induced magnetic field is neglected as the magnetic Reynolds number of the flow is assumed very small. It is further assumed that the external electric field is zero and that the electric field due to charge polarization is negligible. The temperature and the concentration of the ambient fluid are T_∞ *and* C_∞ respectively, while those at the surface are, respectively, $T_w(x)$ and $C_w(x)$.

The pressure gradient, viscous and electrical dissipation are also neglected. The fluid properties are assumed constant, apart from the density in the buoyancy terms of the linear momentum equation, which is estimated using Boussinesq's approximation. Under the above assumptions, the boundary layer form of the governing equation can be written as [10]

$$\frac{\partial u}{\partial x} + \frac{\partial v}{\partial y} = 0 \tag{1}$$

$$u\frac{\partial u}{\partial x} + v\frac{\partial u}{\partial y} = \nu\frac{\partial^2 u}{\partial y^2} + g\beta_T(T - T_\infty) + g\beta_C(C - C_\infty) - \frac{\sigma B_o^2}{\rho}u \tag{2}$$

$$u\frac{\partial T}{\partial x} + v\frac{\partial T}{\partial y} = \alpha\frac{\partial^2 T}{\partial y^2} + \frac{D_m k_T}{c_s c_p}\frac{\partial^2 C}{\partial y^2} \tag{3}$$

$$u\frac{\partial C}{\partial x} + v\frac{\partial C}{\partial y} = D_m\frac{\partial^2 C}{\partial y^2} + \frac{D_m k_T}{T_m}\frac{\partial^2 T}{\partial y^2} \tag{4}$$

The boundary conditions for Eqs. (1)–(4) are expressed as

$$\begin{aligned} &v = V, u = Bx, T = T_w = T_\infty + ax, C = C_w = C_\infty + bx \quad at\ y = 0, \\ &u \to 0, T \to T_\infty, C \to C_\infty \quad as\ y \to \infty, \end{aligned} \tag{5}$$

where B is a constant, a and b denote the stratification rate of the gradient of ambient temperature and concentration profiles and (u, v) are the fluid velocity components in the x and y directions, respectively, Regarding the plate, T is the temperature, β_T is the volumetric coefficient of thermal expansion, α is the

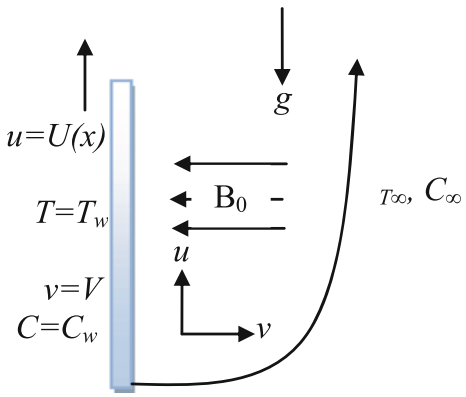

Fig. 1 Physical configuration and coordinate system of the convective heat and mass transfer flow problem. The *horizontal* and *vertical* components of fluid velocity at the plate surface are $U(x)$ and V, respectively

Table 1 Comparisons between the present study and an earlier study (I&M) by Ibrahim and Makinde [7]

Gr	*Gc*	*M*	*Fw*	*Sc*	Present			I&M [7]		
					$-F''(0)$	$-\theta'(0)$	$-\phi'(0)$	$-F''(0)$	$-\theta'(0)$	$-\phi'(0)$
0.1	0.1	0.1	0.1	0.62	0.88908545	0.79653042	0.72547664	0.888971	0.7965511	0.7253292
0.5	0.1	0.1	0.1	0.62	0.69603619	0.83787782	0.76585079	0.695974	0.8379008	0.7658018
1.0	0.1	0.1	0.1	0.62	0.47509316	0.87526944	0.80202587	0.475058	0.8752835	0.8020042
0.1	0.5	0.1	0.1	0.62	0.68702142	0.84207706	0.77016532	0.686927	0.8421370	0.7701717
0.1	1.0	0.1	0.1	0.62	0.45778202	0.88182384	0.80871749	0.457723	0.8818619	0.8087332
0.1	0.1	1.0	0.1	0.62	1.26462533	0.70938977	0.64116350	1.264488	0.7089150	0.6400051
0.1	0.1	3.0	0.1	0.62	1.86838864	0.58541218	0.52519379	1.868158	0.5825119	0.5204793
0.1	0.1	0.1	1.0	0.62	0.57074524	0.56010990	0.52730854	0.570663	0.5601256	0.5271504
0.1	0.1	0.1	3.0	0.62	0.27515400	0.29557231	0.29025308	0.275153	0.2955702	0.2902427
0.1	0.1	0.1	0.1	0.78	0.89351757	0.79373969	0.83398390	0.893454	0.7936791	0.8339779
0.1	0.1	0.1	0.1	2.62	0.91236953	0.78489176	1.65041891	0.912307	0.7847840	1.6504511

$F''(0), \theta'(0)$ and $\phi'(0)$ are determined for various values of embedded parameters with $Pr = 0.72$, $Sr = 0$, and $Du = 0$

Table 2 Computations of $F''(0)$, $\theta'(0)$, and $\phi'(0)$ for various values of embedded parameters

Gr	Gc	M	F_w	Sc	Pr	Sr	Du	$-F''(0)$	$-\theta'(0)$	$-\varphi'(0)$
0.1	0.1	0.1	0.1	0.62	0.72	0.1	0.03	0.88743829	0.78854903	0.69526904
0.5	0.1	0.1	0.1	0.62	0.72	0.1	0.03	0.69354257	0.82992680	0.73536678
1.0	0.1	0.1	0.1	0.62	0.72	0.1	0.03	0.47168842	0.86730429	0.77114416
0.1	0.5	0.1	0.1	0.62	0.72	0.1	0.03	0.68184199	0.83527987	0.74089827
0.1	1.0	0.1	0.1	0.62	0.72	0.1	0.03	0.44921329	0.87564043	0.77968381
0.1	0.1	1.0	0.1	0.62	0.72	0.1	0.03	1.26355437	0.70177349	0.61218037
0.1	0.1	3.0	0.1	0.62	0.72	0.1	0.03	1.86786443	0.57862504	0.49948379
0.1	0.1	0.1	1.0	0.62	0.72	0.1	0.03	0.57021615	0.55630816	0.51327770
0.1	0.1	0.1	3.0	0.62	0.72	0.1	0.03	0.27512619	0.29487694	0.28789907
0.1	0.1	0.1	−0.1	0.62	0.72	0.1	0.03	0.98394287	0.85469292	0.74626691
0.1	0.1	0.1	−1.0	0.62	0.72	0.1	0.03	1.54315969	1.22650204	1.03503982
0.1	0.1	0.1	0.1	0.78	0.72	0.1	0.03	0.89168750	0.78417217	0.79805392
0.1	0.1	0.1	0.1	2.62	0.72	0.1	0.03	0.90971550	0.76190308	1.56957263
0.1	0.1	0.1	0.1	0.62	1.0	0.1	0.03	0.89315322	0.95809716	0.68355351
0.1	0.1	0.1	0.1	0.62	3.0	0.1	0.03	0.90829074	1.75368367	0.63526228
0.1	0.1	0.1	0.1	0.62	7.0	0.1	0.03	0.91639143	2.67686061	0.58104858
0.1	0.1	0.1	0.1	0.62	0.72	0.4	0.03	0.88370546	0.79233598	0.60364269
0.1	0.1	0.1	0.1	0.62	0.72	2.0	0.03	0.86479566	0.81097022	0.10794354
0.1	0.1	0.1	0.1	0.62	0.72	0.1	0.15	0.88598564	0.75328336	0.69792631
0.1	0.1	0.1	0.1	0.62	0.72	0.1	0.60	0.88062396	0.61906425	0.70778467

thermal diffusivity and g is the acceleration due to gravity. Fluid parameters are: υ, the kinematic viscosity; D_m, the coefficient of diffusion in the mixture; C, the species concentration; σ, the electrical conductivity; k_T, the thermal-diffusion ratio; c_s, the concentration susceptibility; c_p, the specific heat at constant pressure and T_m, the mean fluid temperature. B_0 is the externally imposed magnetic field in the y direction. We introduce the following non-dimensional variables:

$$\eta = \sqrt{\frac{B}{\upsilon}}y,\ F(\eta) = \frac{\psi}{x\sqrt{B\upsilon}},\ \theta(\eta) = \frac{T - T_\infty}{T_w - T_\infty},\ \phi(\eta) = \frac{C - C_\infty}{C_w - C_\infty}, \tag{6}$$

where $F(\eta)$ is a dimensionless stream function, $\theta(\eta)$ is a dimensionless temperature of the fluid in the boundary layer region, $\phi(\eta)$ is a dimensionless species concentration of the fluid in the boundary layer region and η is the similarity variable. The velocity components u and v are respectively obtained as follows

$$u = \frac{\partial\psi}{\partial y} = xBF', \quad v = -\frac{\partial\psi}{\partial x} = -\sqrt{B\upsilon}F, \tag{7}$$

where $F_w = \frac{V}{\sqrt{B\upsilon}}$ is the dimensionless suction velocity.

Following Eq. (6), the partial differential equations (2)–(4) are transformed into local similarity equations as follows:

$$F''' + FF'' - (F' + M)F' + G_r\theta + G_c\phi = 0 \tag{8}$$

$$\theta'' + \Pr(F\theta' - F'\theta) + \Pr Du\,\phi'' = 0 \tag{9}$$

$$\phi'' + Sc(F\phi' - F'\phi) + ScSr\,\theta'' = 0, \tag{10}$$

where primes denote differentiation with respect to η. The appropriate flat, free convection boundary conditions are also transformed into the form,

$$\begin{aligned} &F' = 1,\ F = -F_w,\ \theta = 1,\ \phi = 1 \quad at\ \eta = 0 \\ &F' = 0,\ \theta = 0,\ \phi = 0 \quad as\ \eta \to \infty, \end{aligned} \tag{11}$$

where $M = \frac{\sigma B_o^2}{\rho B}$ is the magnetic parameter, $\Pr = \frac{\upsilon}{\alpha}$ is the Prandtl number, $Sc = \frac{\upsilon}{D_m}$ is the Schmidt number, $G_r = \frac{g\beta_T(T_w - T_\infty)}{xB^2}$ is the local temperature Grashof number, $G_c = \frac{g\beta_c(C_w - C_\infty)}{xB^2}$ is the local concentration Grashof number, $D_u = \frac{D_m k_T(C_w - C_\infty)}{c_s c_p(T_w - T_\infty)}$ is the Dufour number, $S_r = \frac{D_m k_T(T_w - T_\infty)}{T_m(C_w - C_\infty)\upsilon}$ is the Soret number.

The quantities of physical interest in this problem are the local skin friction, the local Nusselt number, and the local Sherwood number.

Table 3 Computations of $F''(0)$, $\theta'(0)$, and $\phi'(0)$ for various values of F_w ($Pr=0.72$, $Sc=0.62$, $Gr=0.1$, $Gc=0.1$, $M=0.1$, $Du=0.03$, $Sr=0.1$)

Fw	$-F''(0)$	$-\theta'(0)$	$-\phi'(0)$
0.5	0.724431308	0.67300439	0.60569621
0.3	0.801101962	0.72809519	0.64853672
0	0.934397731	0.82089177	0.72021233
−0.3	1.090853905	0.92677824	0.80186611
−0.5	1.208096735	1.00494205	0.86231477

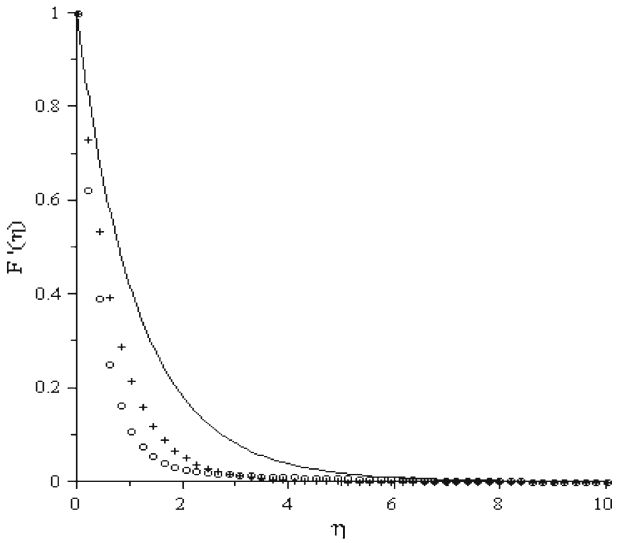

Fig. 2 Velocity profiles of (*continuous line*) $M=0.1$, $F_w=0.1$, (*open circle*) $M=5$, $F_w=0.1$, (*plus symbol*) $M=0.1$, $F_w=-1$ for fixed values of $Pr=0.72$, $Sc=0.62$, $Gr=Gc=0.1$, $Sr=0.1$, $Du=0.03$

3 Numerical Methods for Solution

Equations (8)–(10) constitute a highly non-linear coupled boundary value problem of third and second-order. We converge towards an appropriate η_∞ using a sixth-order Runge–Kutta integration algorithm. We assign an initial guess value for η_∞ and solve the problem with particular parameters to obtain $F''(0)$, $\theta'(0)$ and $\phi'(0)$. The solution process is repeated with a larger value of η_∞ until two successive values of $F''(0)$, $\theta'(0)$ and $\phi'(0)$ lie within a specified limit, signifying the limit of the boundary along η. The final value of η_∞ is used to solve the given set of first-order simultaneous equations in seven unknowns, following the method of superposition [15]. To solve this system we require seven initial conditions whilst we have only two initial conditions, $F'(0)$ and $F(0)$ on F, plus initial conditions on each of θ and φ. Three initial conditions, $F''(0)$, $\theta'(0)\phi'(0)$, are not prescribed. The numerical shooting technique is again employed, using these two ending boundary conditions to produce two unknown initial conditions at $\eta=0$. The calculation assumes step size $\Delta\eta=0.001$, $\eta_{\max}=11$ and five-decimal-place accuracy as the convergence criterion.

4 Results and Discussion

Numerical calculations were made for different values of the thermophysical parameters controlling the fluid dynamics in the flow regime. The values of Schmidt number (*Sc*) are chosen for hydrogen ($Sc=0.22$), water vapor ($Sc=0.62$), ammonia ($Sc=0.78$) and Propyl Benzene ($Sc=2.62$) at temperature 25°C and one atmosphere pressure. The Prandtl number is set as $Pr=0.72$, which represents air at the specified temperature and pressure. Attention is focused on positive values of the buoyancy parameters, i.e. Grashof number $G_r > 0$

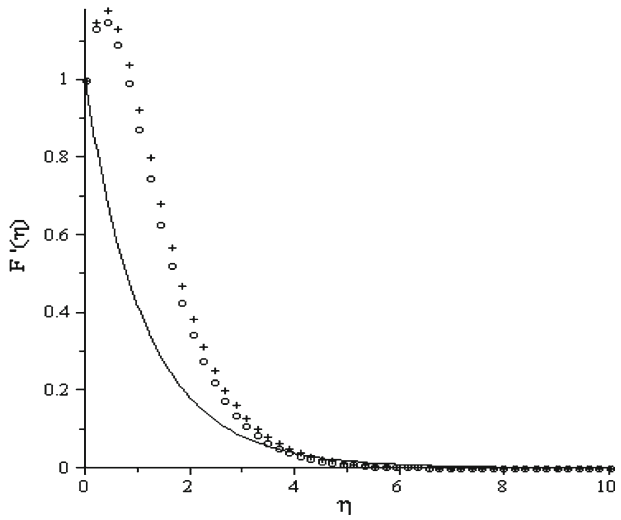

Fig. 3 Velocity profiles of (*continuous line*) $Gr=0.1$, $Gc=0.1$, (*open circle*) $Gr=5$, $Gc=0.1$, (*plus symbol*) $Gr=0.1$, $Gc=5$ for fixed values of $Pr=0.72$, $F_w=0.1$, $M=0.1$, $Sc=0.62$, $Du=0.03$, $Sr=0.1$

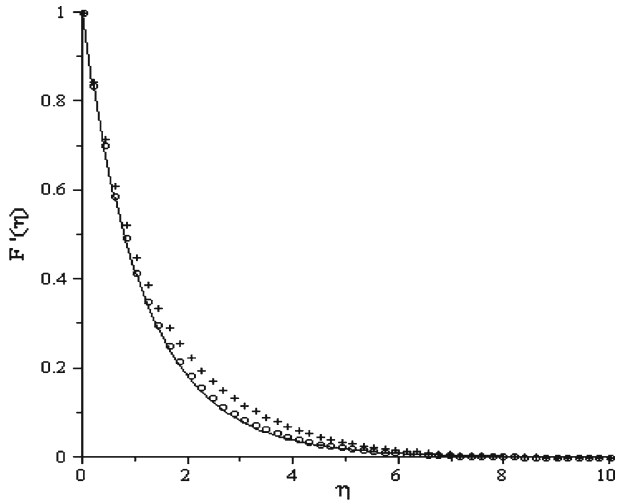

Fig. 4 Velocity profiles of (*continuous line*) $Du=0.03$, $Sr=0.1$, (*open circle*) $Du=0.6$, $Sr=0.1$, (*plus symbol*) $Du=0.03$, $Sr=4$ for fixed values of $Pr=0.72$, $F_w=0.1$, $M=0.1$, $Sc=0.62$, $Gr=Gc=0.1$

(corresponding to the cooling problem) and solutal Grashof number $G_c > 0$ (which indicates that the chemical species concentration in the free stream region is less than its concentration at the boundary surface). The cooling problem is frequently encountered in engineering applications; for example, in the cooling of electronic components and nuclear reactors. In all computations we seek F, θ and ϕ as functions of η for the velocity, temperature and species diffusion boundary layers. Table 1 shows comparisons between the present work and that of an earlier study by Ibrahim and Makinde [7] for Prandtl number ($Pr=0.72$), and the perfect agreement in the absence of Dufour and Soret is worthy of note. From Table 2, it is seen that the local skin friction together with the heat and mass transfer rate at the moving plate surface decreases with increasing magnitude of fluid suction (F_w) at the moving surface, while the local skin-friction, mass and heat transfer increases with decreasing magnitude of fluid injection at the moving surface. The rate of heat and mass transfer at the plate surface increases with increasing intensity of buoyancy forces (*Gr, Gc*), but decreases with increasing intensity of magnetic field (M), and with increasing Dufour and Soret numbers (*Du, Sr*). Moreover, the skin friction decreases with buoyancy forces and increases as the magnetic field intensity and Schmidt number (*Sc*) increase. Finally, we observed that the flow field is appreciably influenced by the Dufour and Soret effects. Hence we conclude that for fluids of hydrogen-air mixtures, the Dufour and Soret effects should not be neglected. Furthermore, increasing the Schmidt number causes the surface mass transfer rate and the surface heat transfer rate

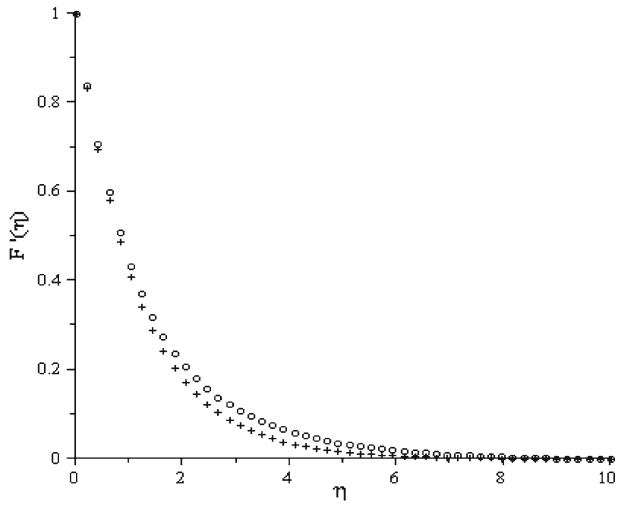

Fig. 5 Velocity profiles of (*plus symbol*) $Pr=0.72$, $Du=0$, $Sr=0$, (*open circle*) $Pr=0.72$, $Du=0.6$, $Sr=2$ for $M=Gr=Gc=F_w=0.1$, $Sc=0.62$

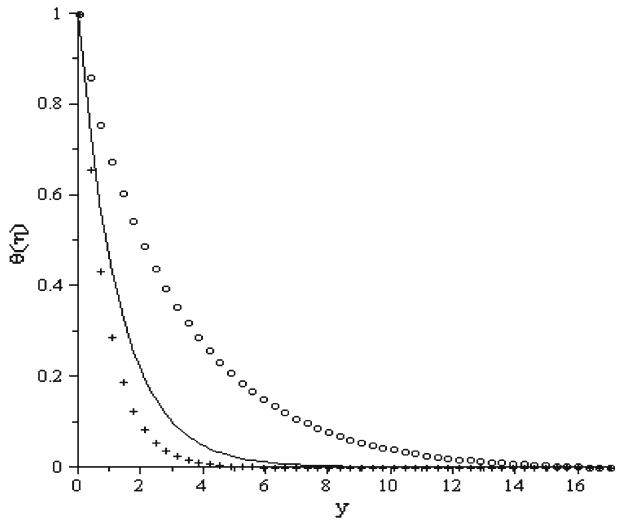

Fig. 6 Temperature profiles of (*continuous line*) $M=0.1$, $F_w=0.1$, (*open circle*) $M=5$, $F_w=0.1$, (*plus symbol*) $M=0.1$, $Fw=-1$ for fixed values of $Pr=0.72$, $Sc=0.62$, $Gr=Gc=0.1$, $Sr=0.1$, $Du=0.03$

to increase and decrease, respectively. From Table 3, we observe that the suction parameter ($F_w > 0$) tends to increase the local skin friction, while the opposite trend is observed for the injection parameter ($F_w < 0$). This occurs because blowing gives rise to a thicker velocity boundary layer, thereby causing a decrease in the velocity gradient at the surface. The local Nusselt number increases for negative values of the suction parameter, and decreases for positive values of the injection parameter. Applying the injection at the surface reduces the momentum transport near the surface, thereby causing a decrease in the local Nusselt number. Similarly, the local Sherwood number increases in the presence of the suction parameter, and decreases in the presence of the injection parameter.

4.1 Velocity Profiles

Figures 2, 3, 4 and 5 depict the effects of emerging flow parameters on non-dimensional velocity profiles. In Fig. 2 the effect of magnetic field strength and injection suction parameter on the momentum boundary-layer thickness is illustrated. Increasing the magnetic field strength parameter induces a decrease in the velocity as expected, given that the magnetic field creates a drag force that opposes the fluid motion, and therefore

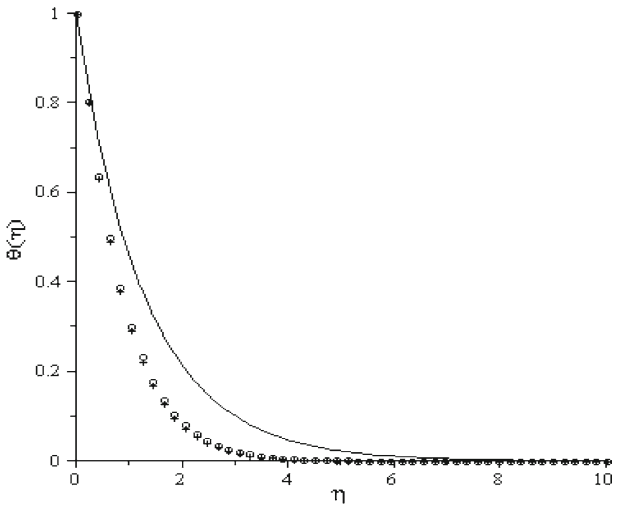

Fig. 7 Temperature profiles of (*continuous line*) $Gr=0.1$, $Gc=0.1$, (*open circle*) $Gr=5$, $Gc=0.1$, (*plus symbol*) $Gr=0.1$, $Gc=5$ for fixed values of $Pr=0.72$, $F_w=0.1$, $M=0.1$, $Sc=0.62$, $Du=0.03$, $Sr=0.1$

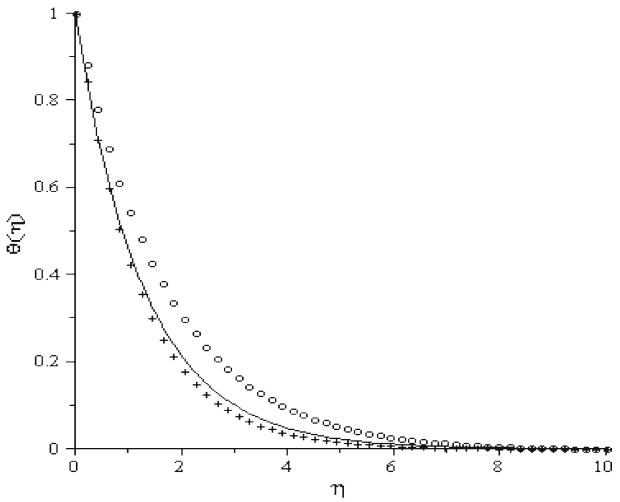

Fig. 8 Temperature profiles of (*continuous line*) $Du=0.03$, $Sr=0.1$, (*open circle*) $Du=0.6$, $Sr=0.1$, (*plus symbol*) $Du=0.03$, $Sr=4$ for fixed values of $Pr=0.72$, $F_w=0.1$, $M=0.1$, $Sc=0.62$, $Gr=Gc=0.1$

dampens the velocity. Figure 2 also reveals that fluid velocity within the boundary layer increases because of suction, and decreases because of injection. This is consistent with the established fact that suction stabilizes the boundary layer growth. Furthermore, as shown in Fig. 3, an increase in the buoyancy forces parameters leads to an increase in the velocity profile. High buoyancy forces are known to enhance fluid flow. In Fig. 4, it is apparent that increases in Soret and Dufour numbers (corresponding to increases in fluid flow) cause the momentum boundary layer thickness to increase. Figure 5 shows the comparison between [7] and the present study for $Du=0$, $Sr=0$ and $Du=0.6$, $Sr=2$. The graph clearly shows that incorporating the Soret and Dufour numbers increases the thickness of the velocity boundary layer across the plate.

4.2 Temperature Profiles

The effects of various thermophysical parameters on the fluid temperature are illustrated in Figs. 6, 7, 8, 9, 10. Generally, the fluid temperature increases from the plate surface and is maximized at the free stream whenever

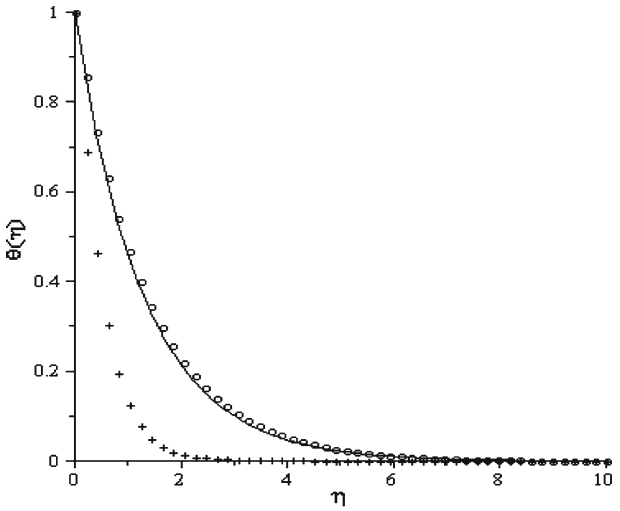

Fig. 9 Temperature profiles of (*continuous line*) $Sc=0.62$, $Pr=0.72$, (*open circle*) $Sc=2.62$, $Pr=0.72$, (*plus symbol*) $Sc=0.62$, $Pr=3$ for fixed values of $F_w=0.1$, $M=0.1$, $Gr=Gc=0.1$, $Du=0.03$, $Sr=0.1$

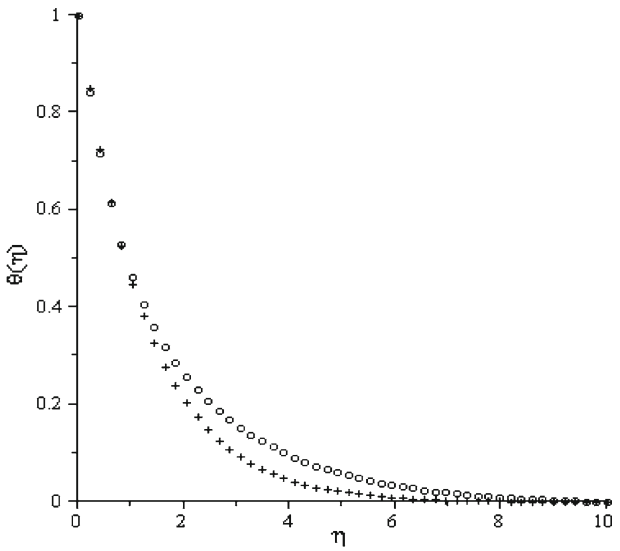

Fig. 10 Temperature profiles of (*plus symbol*) $Pr=0.72$, $Du=0$, $Sr=0$, (*open circle*) $Pr=0.72$, $Du=0.6$, $Sr=2$ for $M=Gr=Gc=F_w=0.1$, $Sc=0.62$

the plate surface temperature θ_w is lower than the free stream temperature. Figure 6 illustrates the influence of magnetic field strength and the suction parameter on the temperature profile of the fluid boundary layer. It is clearly seen that increasing the magnetic field strength increases the thermal boundary layer thickness across the plate, while increasing the suction parameter decreases the temperature of this layer. In Fig. 7, we observe that an increase in both thermal and solutal Grashof number induces a decrease in the fluid temperature while increasing the buoyancy forces. Figure 8 shows the influence of Dufour and Soret numbers on fluid temperature. Increasing the Dufour and Soret numbers causes the fluid temperature to increase and decrease, respectively. The effect of Schmitz number and Prandtl number is illustrated in Fig. 9. Here, we observe that increasing the Prandtl number causes the thermal boundary layer thickness to increase, thereby increasing the fluid temperature. The Schmitz number exerts little influence on the fluid temperature. Figure 10 illustrates the comparison between [7] and the present study for two choices of Du and Sr, namely, $Du=0$, $Sr=0$ and $Du=0.6$, $Sr=2$. From this figure, it is apparent that incorporation of the Soret and Dufour numbers increases the thickness of the thermal boundary layer across the plate.

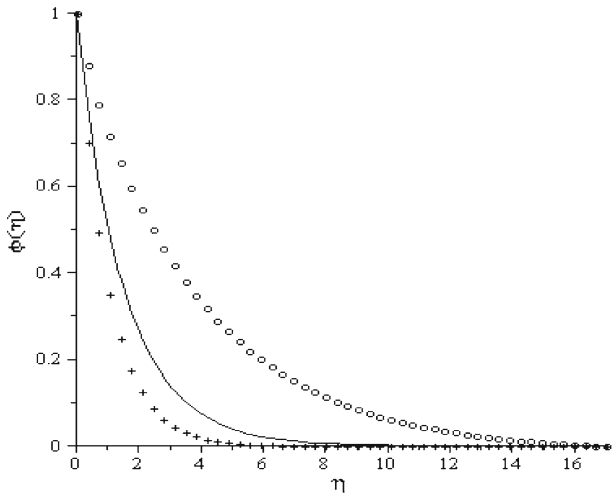

Fig. 11 Concentration profiles of (*continuous line*) $M=0.1$, $F_w=0.1$, (*open circle*) $M=5$, $F_w=0.1$, (*plus symbol*) $M=0.1$, $F_w=-1$ for fixed values of $Pr=0.72$, $Sc=0.62$, $Gr=Gc=0.1$, $Sr=0.1$, $Du=0.03$

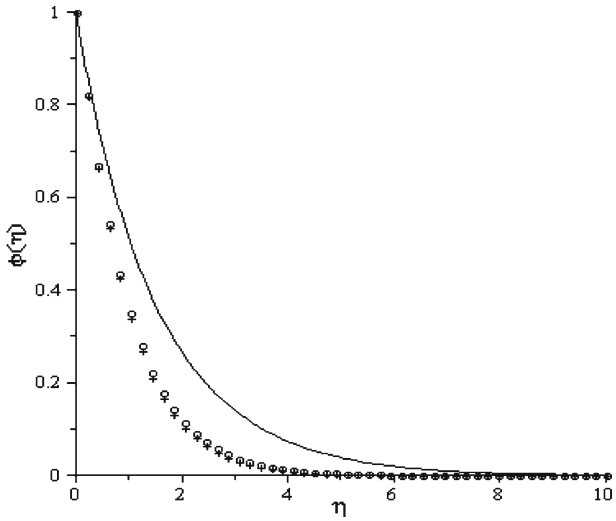

Fig. 12 Concentration profiles of (*continuous line*) $Gr=0.1$, $Gc=0.1$, (*open circle*) $Gr=5$, $Gc=0.1$, (*plus symbol*) $Gr=0.1$, $Gc=5$ for fixed values of $Pr=0.72$, $F_w=0.1$, $M=0.1$, $Sc=0.62$, $Du=0.03$, $Sr=0.1$

4.3 Concentration Profiles

Figures 11, 12, 13, 14, 15 depict chemical species concentration profiles as functions of η for varying values of physical parameters in the boundary layer. It is noteworthy that the species concentration increases from the plate surface and attains its peak value at free stream whenever the concentration at the plate surface ϕ_w is lower than that of the free stream. Figure 11 shows the influence of the magnetic field strength and suction parameter on species concentration. Increasing the magnetic field strength causes the thickness of the species concentration boundary layer to increase, while increasing the injection parameter induces the opposite effect, with subsequent decaying of concentration boundary layer thickness. The concentration boundary layer thickness across the plate also decreases as the thermal and solutal Grashof numbers increase, as shown in Fig. 12. In Fig. 13, we observe an increase in concentration boundary layer thickness as the Soret number increases, while little or no effect occurs with increase in Dufour number. Figure 14 illustrates the influence of Schmidt and Prandtl numbers on the species concentration. Here it is seen that increasing the Schmidt number decreases the species concentration within the boundary layer, due to the combined effects of buoyancy forces and species

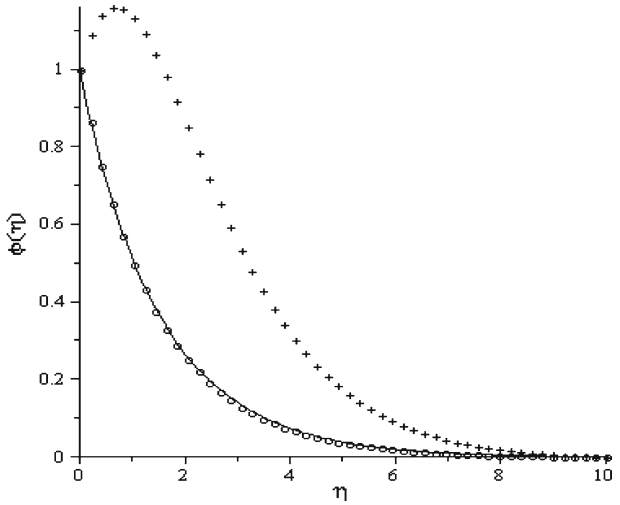

Fig. 13 Concentration profiles of (*continuous line*) $Du=0.03$, $Sr=0.1$, (*open circle*) $Du=0.6$, $Sr=0.1$, (*plus symbol*) $Du=0.03$, $Sr=4$ for fixed values of $Pr=0.72$, $F_w=0.1$, $M=0.1$, $Sc=0.62$, $Gr=Gc=0.1$

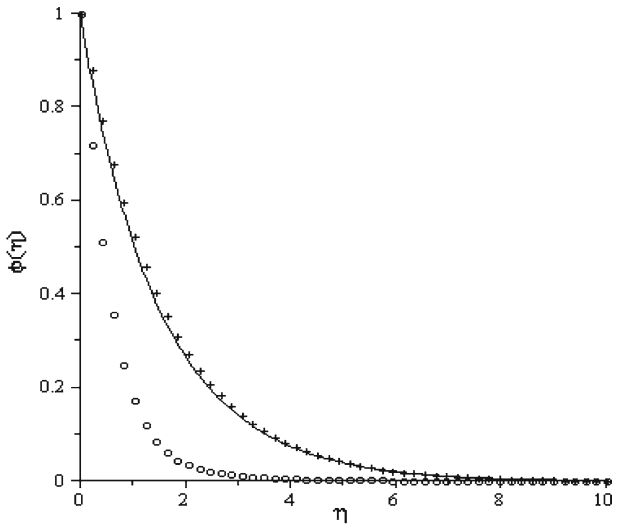

Fig. 14 Concentration profiles of (*continuous line*) $Sc=0.62$, $Pr=0.72$, (*open circle*) $\mathrm{Sc}=2.62$, $Pr=0.72$, (*plus symbol*) $Sc=0.62$, $Pr=3$ for fixed values of $F_w=0.1$, $M=0.1$, $Gr=Gc=0.1$, $Du=0.03$, $Sr=0.1$

molecular diffusivity. The effects of Dufour and Soret numbers on the species concentration boundary layer thickness for the two parameter sets $Pr=0.72$, $Du=0$, $Sr=0$ and $Pr=0.72$, $Du=0.6$, $Sr=2$ are revealed in Fig. 15. It becomes apparent that the effects of these two parameters on concentration boundary layer thickness cannot be under estimated.

5 Conclusions

In this paper, we have investigated MHD free convective heat and mass transfer past a moving vertical plate with Soret and Dufour effect in the presence of suction/injection parameters. The effects of thermal-diffusion and diffusion thermo with suction/injection parameter are evaluated. Similarity solutions are obtained using scaling transformations. The set of governing equations and the boundary conditions are reduced to ordinary differential equations with appropriate boundary conditions. Influence of Soret number, Dufour number, suction/injection parameter, Schmidt number, Prandtl number and magnetic parameter on MHD free convective heat and mass transfer have been explored in detail. The skin friction coefficient and the local Nusselt number were found to

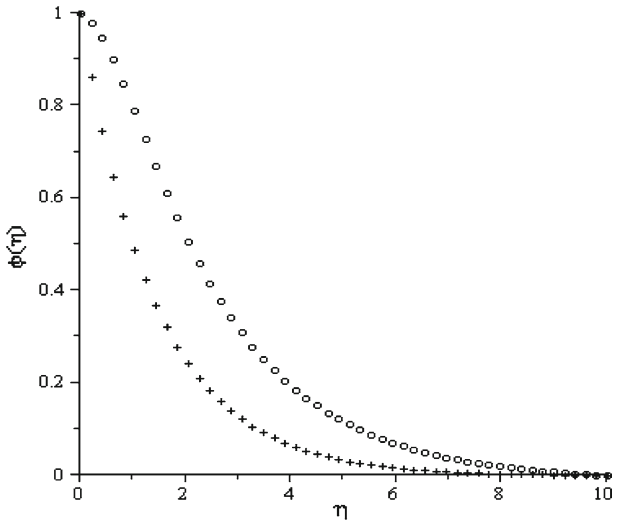

Fig. 15 Concentration profiles of (*plus symbol*) $Pr=0.72$, $Du=0$, $Sr=0$, (*open circle*) $Pr=0.72$, $Du=0.6$, $Sr=2$ for $M=Gr=Gc=F_w=0.1$, $Sc=0.62$

decrease with increasing Dufour number and with decreasing Soret number, respectively. Excellent agreement between the study and that of Ibrahim and Makinde [7] was obtained. Finally, in the presence of a magnetic field, the fluid velocity around the plate was observed to decrease, associated with a reduction of the velocity gradient at the wall, and the local skin-friction coefficient decreased accordingly. Similarly, we noted a decrease in the wall temperature gradient and concentration gradient in the presence of a magnetic field, reflected as a decrease in the local Nusselt and Sherwood numbers.

Acknowledgments The authors wish to thank Covenant University, Ota, Nigeria for financial support.

References

1. Alam, M.S.; Rahman, M.M.: Dufour and Soret effects on mixed convection flow past a vertical porous flat plate with variable suction. Nonlinear Anal. Model. Control **11**(1), 3–12 (2006)
2. Beg, A.O.; Bakier, A.Y.; Prasad, V.R.: Numerical study of free convection magnetohydrodynamic heat and mass transfer from a stretching surface to a saturated porous medium with Soret and Dufour effects. Comput. Mater. Sci. **46**, 57–65 (2009)
3. Bejan, A.; Dincer, I.; Lorente, S.; Miguel, A.F.; Reis, A.H.: Porous and complex flow structures in modern technologies. Springer, New York (2004)
4. Chakrabarti, A.; Gupta, A.S.: Hydromagnetic flow and heat transfer over a stretching sheet. Q Appl. Math. **37**, 73–78 (1979)
5. Chiam, T.C.: Hydrodynamic flow over a surface stretching with a power law velocity. Int. J. Eng. Sci. **33**, 429–435 (1995)
6. Gaikwad, S.N.; Malashetty, M.S.; Prasad, K.R.: An analytical study of linear and non-linear double diffusive convection with Soret and Dufour effects in couple stress fluid. Int. J. NonLinear Mech. **42**, 903–913 (2007)
7. Ibrahim, S.Y.; Makinde, O.D.: Chemically reacting MHD boundary layer flow of heat and mass transfer past a moving vertical plate with suction. Sci. Res. Essay **5**(19), 2875–2882 (2010)
8. Ingham, D.B.; Bejan, A.; Mamut, E.; Pop, I.: Emerging technologies and techniques in porous media. Kluwer, Dordrecht (2004)
9. Ingham, D.B.; Pop, I.: Transport phenomena in porous media, vol. III. Pergamon, Oxford (2005)
10. Kafoussias, N.G.; Williams, E.W.: Thermal-diffusion and diffusion-thermo effects on mixed free-convective and mass transfer boundary layer flow with temperature dependent viscosity. Int. J. Eng. Sci. **33**, 1369–1384 (1995)
11. Makinde, O.D.: MHD steady flow and heat transfer on the sliding plate. A.M.S.E. Model. Meas. Control B. **70**(1), 61–70 (2001)
12. Makinde, O.D.: Magneto-hydrodynamic stability of plane-Poiseuille flow using multi-deck asymptotic technique. Math. Comput. Model. **37**(3–4), 251–259 (2003)
13. Makinde, O.D.: Effect of arbitrary magnetic Reynolds number on MHD flows in convergent-divergent channels. Int. J. Numer. Methods Heat Fluid Flow **18**(6), 697–707 (2008)
14. Makinde, O.D.: On MHD boundary-layer flow and mass transfer past a vertical plate in a porous medium with constant heat flux. Int. J. Num. Methods Heat Fluid Flow **19**(3/4), 546–554 (2009)
15. Na, T.Y.: Computational methods in engineering boundary value problems. Academic Press, New York (1979)
16. Nield, D.A.; Bejan A.: Convection in porous media, 3rd edn. Springer, New York (2006)
17. Nithyadevi, N.; Yang, R.-J.: Double diffusive natural convection in a partially heated enclosure with Soret and Dufour effects. Int. J. Heat Fluid Flow (2009, in press)

18. Olanrewaju, P.O.: Dufour and soret effects of a transient free convective flow with radiative heat transfer past a flat plate moving through a binary mixture. Pac. J. Sci. Technol. **11**(1), 163–172 (2010)
19. Osalusi, E.; Side, J.; Harris, R.: Thermal-diffusion and diffusion-thermo effects on combined heat and mass transfer of a steady MHD convective and slip flow due to a rotating disk with viscous dissipation and Ohmic heating. Int. Commun. Heat Mass Transf. **35**, 908–915 (2008)
20. Pop, I.; Ingham, D.B.: Convective heat transfer: mathematical and computational modeling of viscous fluids and porous media. Pergamon, Oxford (2001)
21. Sakiadis, B.C.: Boundary layer behavior on continuous solid surfaces I. Boundary layer equations for two-dimensional and axisymmetric flow. AICHE J. **7**, 26–28 (1961)
22. Sparrow, E.M.; Cess, R.D.: The effect of a magnetic field on free convection heat transfer. Int. J. Heat Mass Transf. **4**, 267–274 (1961)
23. Vadasz, P: Emerging topics in heat and mass transfer in porous media. Springer, New York (2008)
24. Vafai, K: Handbook of porous media. Taylor & Francis, New York (2005)
25. Yih, K.A.: Free convection effect on MHD coupled heat and mass transfer of a moving permeable vertical surface. Int. Commun. Heat Mass Transf. **26**(1), 95–104 (1999)